Journal of Magnetism and Magnetic Materials 427 (2017) 60–66

Contents lists available at ScienceDirect

Journal of Magnetism and Magnetic Materials

journal homepage: www.elsevier.com/locate/jmmm

Size-dependent cytotoxicity and inflammatory responses of PEGylated silica-iron oxide nanocomposite size series☆

Wishulada Injumpa[a], Patcharee Ritprajak[b], Numpon Insin[a,*]

[a] Department of Chemistry, Faculty of Science, Chulalongkorn University, Bangkok 10330, Thailand
[b] Department of Microbiology, and RU in Oral Microbiology and Immunology, Faculty of Dentistry, Chulalongkorn University, Bangkok 10330, Thailand

ARTICLE INFO

Keywords:
Magnetic nanoparticles
Nanocomposites
Silica
PPEGMA
Inflammatory
Magnetite

ABSTRACT

Iron oxides nanoparticles have been utilized in biological systems and biomedical applications for many years because they are relatively safe and stable comparing to other magnetic nanomaterials. In some applications, iron oxide nanoparticles were modified with silica in order to be more stable in biological systems and able to be functionalized with various functional groups. Moreover, poly(ethylene glycol) (PEG) was one on the most used polymer to graft onto the nanoparticles in order to increase their biocompatibility, dispersibility and stability in aqueous solutions. Therefore, the nanocomposites comprising iron oxide nanoparticles, silica, and PEG could become multifunctional carriers combining superparamagnetic character, multi-functionality and high stability in biological environments. Herein, we reported the preparation of the nanocomposites and effects of their sizes on cytotoxicity and inflammatory responses.

The PEGylated silica-iron oxide nanocomposites were prepared by coating of poly(poly(ethylene glycol) monomethyl ether methacrylate) (PPEGMA) on magnetic nanoparticle-silica nanocomposites *via* Atom Transfer Radical Polymerization (ATRP). The iron oxide nanoparticles were synthesized using a thermal decomposition method. The silica shells were then coated on iron oxides nanoparticles using reverse microemulsion and sol-gel methods. The size series of the nanocomposites with the diameter of 24.86 ± 4.38, 45.24 ± 5.00, 98.10 ± 8.88 and 202.22 ± 6.70 nm as measured using TEM were obtained. Thermogravimetric analysis (TGA) was used for the determination of % weight of PPEGMA on the nanocomposites showing the weight loss of ranging from 65% for smallest particles to 30% for largest particles. The various sizes (20, 40, 100, 200 nm) and concentrations (10, 100, 1000 μg/mL) of the nanocomposites were tested for their cytotoxicity in fibroblast and macrophage cell lines using MTT assay. The different sizes did not affect cell viability of fibroblast, albeit incubation with the highest concentration of 1000 μg/mL. Although 1000 μg/mL of all sizes of the nanocomposites decreased macrophage viability, the cytotoxicity of the nanocomposites was notably less than silica. The inflammatory response of macrophage was also observed by ELISA, and we found that the size of 20 and 40 nm, but not 100 and 200 nm, obviously stimulated IL-6 production. From this study, the preparations of multifunctional superparamagnetic nanocomposites of different sizes along with the size-dependent effects on cellular toxicity and inflammatory response were demonstrated and could be applied for designing of new drug carriers.

1. Introduction

Magnetic nanoparticles (MNPs) have been of interest in many fields because of their superparamagnetic character and large surface area. Especially, they were emerged in therapeutic applications such as tumor and lesion therapy under external magnetic fields. Magnetic iron oxides, magnetite and maghemite, are among the most used as they showed less toxic side effects on normal cells.[1] MNPs usually need stabilizers to prevent their aggregation and improve their stability in water-based solutions. General, MNPs was coated with biocompatible materials and can be regarded as magnetic nanocomposites (MNCs) in order for the MNPs to become useful in biological application. The coating materials include stable and low toxic inorganic materials and biocompatible polymers.

Silica is among biocompatible inorganic materials that has been widely used as coating materials because not only the stability in physiological environment, but it can also be easily functionalized and become multifunctional materials.[2–4] Silica has been utilized as

☆ In remembrance of His Majesty King Bhumibol Adulyadej (1927–2016), for his life-time dedication to Thailand.

* Corresponding author.
E-mail address: Numpon.I@chula.ac.th (N. Insin).

http://dx.doi.org/10.1016/j.jmmm.2016.11.015
Received 25 June 2016; Received in revised form 20 October 2016; Accepted 1 November 2016
Available online 05 November 2016
0304-8853/

carriers for drug and biomolecule delivery systems. As magnetic nanoparticle coating, silica-coated iron oxides nanoparticles were reported to exhibit high stability, large surface area and various functional groups modified onto the surface.[5,6].

For polymer coating on nanomaterials, polymers are considered as good stabilizers because of the large molecular weight and structure with long chain that could prevent agglomeration and aggregation of nanomaterials. Wide selections of polymers, such as degradable polymers, pH and environmental sensitive polymers, and hydrophilic polymers (cationic, anionic and non-ionic polymers), were investigated depending on the required properties for the specific systems. For MNPs coating, poly(ethylene glycol) (PEG) was extensively used as coating materials because the PEG-coated MNPs could become injectable and biocompatible materials for biological studies.[1,7,8].

In the applications of synthetic nanomaterials in biological research, one of the most important factors to be considered is low toxicity level after the materials were exposed with cells, tissues, and organisms.[9–11] It has been reported that the size of nanomaterials carriers evidently affected the biological responses and is of important factor to consider in biological applications.[12] In animal body, it has been observed that some cells took up particles and unknown molecules of specific size ranges.[13] Also, stabilities, lifetime, and handlings of particles were size-dependent.[14,15] For magnetic nanocomposites, MNCs in size range of 10–50 nm were used to carry dyes and drugs for *in vivo* delivery studies,[8,16] while MNCs in size range of 10–20 nm were applied as carriers for cellular imaging and DNA hybridization.[17,18]. In the size range of 10–200 nm, MNCs were used as carriers for *E. coli* isolation, and approximately, MNCs with 250 nm in diameter were used as carriers for targeting thrombolysis with recombinant tissue plasminogen activator.[19–21] From the previous works mentioned, it was obvious that the MNCs, with the different coating depending on the functions needed, with the size ranging from 10 to 250 nm are crucial for many experiments in biological systems.

In this work, we are interested in preparation of MNCs that combine iron oxides nanoparticle, silica, and PEG, the three materials that were applied in biological research extensively, into nanocomposites with specific sizes ranging from 20 to 200 nm in diameter. Iron oxides MNCs prepared using hydrothermal method, and then they were formed nanocomposites with silica using sol-gel chemistry. The poly(poly(ethylene glycol) methacrylate) were then grafted onto the silica coating using Atom Transfer Radical Polymerization (ATRP) to attach the PEG entity onto the MNCs. The cytotoxicity and inflammatory responses upon stimulation with MNCs of different sizes were investigated. The methods for preparation of iron oxides-silica-PEG MNCs and the effects of their sizes on the cytotoxicity and inflammatory responses could be essential information for further biological applications of these groups of materials.

2. Materials and methods

All chemicals were used as received without further purification. Iron (III) chloride ($FeCl_3$) (99.99%), oleic acid (90%), 1-octadecene (90%), ammonium fluoride, sodium hydroxide (pellet for analysis), Tetraethyl orthosilicate (TEOS; purum > 98%), ammonium hydroxide (NH_4OH; 25%), polyoxyethylene (5) nonylphenylether (Igepal CO-520), Triton X-100 (laboratory grade), 5-amino-pentanol (AP; reagent grade), 3-aminopropyltriethoxysilane (APS), 12-hydroxydodecanoic acid (HDC; reagent grade), 2-bromoisobutyl bromide (BiBB), Copper(I) bromide (CuBr; 99.99%), N,N,N′,N′′,N′′-Pentamethyldiethylenetriamine (PMDTA; reagent grade) and poly(ethylene glycol) monomethyl ether methacylate (PEGMA; Mn 360) were purchased from Sigma-Aldrich.

2.1. Synthesis of magnetic nanoparticles (MNPs)

Thermal decomposition technique was used for the syntheses of magnetite (Fe_3O_4) NPs or MNPs with a process previously reported with some modifications.[22] $Fe(oleate)_3$ was firstly prepared as a precursor from iron (III) chloride and oleic acid. In the $Fe(oleate)_3$ preparation, 8 mmol of iron (III) chloride was dissolved in 10 mL of de-ionized (DI) water, and 24 mmol of sodium hydroxide was dissolved in 10 mL of DI water. Then 24 mmol of oleic acid and the sodium hydroxide solution were added into a round bottom flask, yielding the sodium oleate solution. Finally, iron (III) chloride solution and a mixture of DI water: ethanol:hexane in the ratio of 12:16:28 by volume (mL) were added into the oleate solution. The mixture was refluxed at 70 °C for 4 h. Then, the mixture was extracted by three times of 6.0 mL of DI water. $Fe(oleate)_3$ was then dispersed in the hexane layer. The $Fe(oleate)_3$ dispersion was collected and was evaporated to obtain the $Fe(oleate)_3$ as dark brown fluid. For the step of the synthesis of MNPs by thermal decomposition process, a mixture of oleic acid : $Fe(oleate)_3$: 1-octadecence of 1.0 : 6.0 : 38 by mole was prepared. The mixture was gradually heated as controlled by a temperature controller to 320 °C with the heating rate of 3.3 °C/min, and the reaction mixture was held at this temperature for 30 min under inert atmosphere (N_2 gas). MNPs dispersion were then collected after washed for several times by 2-propanol using a centrifuge.

2.2. Synthesis of core-shell magnetite-silica magnetic nanocomposites (M@S MNCs)

To begin with the preparation of reverse micelles,[23] 84 mL of cyclohexane and 9.8 g polyoxyethylene (5) nonylphenylether (Igepal CO-520) were mixed using a magnetic stirrer until obtaining a clear mixture. Then 0.8 mL of 110 mg/mL magnetite in cyclohexane dispersion was added in the reverse micelle mixture. Next, 1.5 mL of 25% ammonium hydroxide was added following by continuous stirring for 10 min. At the last step, 0.6 and 3.0 mL of tetraethylorthosilicate (TEOS) were added dropwise depending on the silica thickness, and the reaction was kept stirring for 16 h. M@S MNCs were then obtained and washed for three times with 30 mL of ethanol before kept for later used.

2.3. Synthesis of magnetite-decorating silica particles (S-M MNCs)

2.3.1. Synthesis of bare silica NPs

A reverse emulsion was used for the synthesis of bare silica NPs. The emulsion was prepared by mixing 25.0–37.5 mL of poly(ethylene glycol) tert-octylphenyl ether (Triton X-100), 16.0–24.0 mL of 1-hexanol and 75.0 mL of cyclohexane.[24] The mixtures were mixed by sonication for 30 min. Then, 6.00 mL of DI water was added into the mixtures. The mixtures were stirred until clear. 1.25 mL of 25% NH_4OH was then added into the emulsion. After stirring for 2 h, 3.9 and 4.2 mL of TEOS (depending on the expected sizes of the silica nanoparticles) were added as a silica source. Finally, bare silica NPs were obtained after the emulsion was stirred for 24 h and washed by centrifugation-precipitation for three times with 30 mL of ethanol.

2.3.2. Preparation of ethanolic magnetite dispersion

As-synthesized magnetite NPs were removed of the excess surfactants using repeated centrifugation-redispersion in ethanol from more than three times. In order to become attachable onto bare silica surfaces, free magnetite NPs were then modified with multifunctional ligand systems [25]. For the modification, 35 mg of dried magnetite NPs was dispersed in 0.50 mL of ethanol. Then, 95 mg of 12-hydroxydodecanoic acid (HDC) was added into the magnetite dispersion. Then, the dispersion was sonicated for 30 min or until the dispersion becoming clear before the addition of 415 mg of 5-amino-pentanol (AP) and 400 mg of 3-aminopropyltriethoxysilane (APS). The mixture

was stirred for 20 min, and the ethanolic magnetite dispersion as a clear brown solution was observed.

*2.3.3. Preparation of magnetite NPs on silica particles (*S-M MNCs*)*

100 mg of bare silica NPs was dispersed in 120 mL of ethanol, and then 0.4–0.6 mL of MNPs dispersion in ethanol was added dropwise into the dispersion. The mixture was stirred for 20 min before 0.1 mL of DI water and 0.1 mL of 25% NH_4OH were added, respectively. After 5 min, 0.2 mL of TEOS was added into the dispersion, and then the dispersion was continuously stirred for another 16 h. After washed for three times with 30 mL of ethanol, S-M MNCs were obtained [25].

2.4. Preparation of Poly(poly(ethylene glycol)monomethyl ether methacylate) (PPEGMA)-coated on the nanocomposites

The preparation of all of PPEGMA-coated on MNCs was divided into 3 steps. In the first steps, all of MNCs were functionalized with 3-aminopropyltriethoxysilane (APS) to obtain amino group on MNCs (MNC-NH_2.) Then, the MNC-NH_2 was immobilized with ATRP initiator (BiBB) and formed bromide group on MNCs surface (MNC-Br.) In the last step, MNC-Br was coated with PPEGMA by the polymerization of PEGMA, and Poly(poly(ethylene glycol)monomethyl ether methacylate) (PPEGMA)-coated MNCs (MNC@PPEGMA) of different sizes were obtained [24].

2.4.1. NH_2-functionalization on S-M and M@S MNCs surface

250 mg of M@S and S-M MNCs were dispersed in 100 mL of 2-propanol, and 2.00 mL of APS was then added dropwise. The mixture was continuously stirred for 24 h to get M@S-NH_2 or S-M-NH_2 MNCs. Before used in the next steps, the MNCs were washed with 25 mL of 2-propanol (×2) and 25 mL of dichloromethane (×2), respectively [24].

2.4.2. Initiator-functionalization on S-M-NH_2 and M@S-NH_2 MNCs surfaces

300 mg of S-M-NH_2 and M@S-NH_2 MNCs were dispersed in 30 mL of dichloromethane. 1 mL of triethylamine was added into the dispersion. The dispersion was immersed into an ice bath under nitrogen atmosphere. After 10 min, 0.3 mL of 2-bromoisobutylylbromide (BiBB) was added dropwise. The mixture was stirred at 0 °C for 2 h under N_2 gas and then continuously stirred for another 20 h at room temperature. Before used in the next step, S-M-NH_2-Br and M@S-NH_2-Br MNCs were washed with 30 mL of dichloromethane for 3 times, 30 mL of ethanol twice and 30 mL of water twice, respectively [24].

2.4.3. Synthesis of PPEGMA-coated on S-M-Br and M@S-Br MNCs surface

300 mg of S-M-Br or M@S-Br MNCs were dispersed into mixed solution of 5 mL of DI water and 30 mL of methanol. The dispersion was immersed into an ice bath and magnetically stirred. Then the atmosphere above the dispersion was pumped-refilled with N_2 for 3 cycles. 2 mL of the monomer PEGMA was added dropwise into the dispersion before 0.1 mg of copper (I) bromide and 1 mL of N,N,N′,N′′,N′′-pentamethyl-diethylenetriamine (PMDETA) were added, respectively. After that, the mixture was stirred under N_2 for 16 h. After washed with 30 mL of ethanol for 3 times, 30 mL of methanol twice and 30 mL of DI water twice, S-M@PPEGMA and M@S@PPEGMA MNCs were obtained. The samples were then collected and kept in DI water [24].

2.5. Materials analyses

X-ray diffraction (XRD) patterns of samples were obtained on a DMAX 2200/Ultima+diffractometer (Rigaku, Tokyo, Japan) using Cu Kα radiation source and operating at 40 kV and 30 mA. The XRD spectra were collected with a scan range of 20–70° and scan speed of 1°/min. Transmission electron microscopy (TEM) photographs of particles were obtained using a JEM-2010 microscope at accelerating voltage of 120 kV (Japan). The dispersed samples of MNPs and MNCs were deposited on carbon films with 300 mesh copper grids, and then dried in desiccators at room temperature. The average size was then estimated from several obtained TEM images using ImageJ program. Fourier-transform infrared (FTIR) spectra were acquired using a Nicolet 6700 (Thermo Scientific, MA, USA).

2.6. In vitro *cytotoxicity*

The *in vitro* cytotoxicity was measured on macrophage (RAW264.7) or fibroblast (L9296) cell lines using 3-(4,5-dimethylthiazol-2-yl)-2,5-diphenyltetrazolium bromide (MTT) assay [26]. The cells were cultured in DMEM media (GIBCO, Invitrogen, CA, USA) supplemented with 10% FBS (GIBCO, Invitrogen, CA, USA), 100 U/mL penicillin and 100 μg/mL streptomycin (Hyclone, GE Healthcare Life Science, UT, USA), 4 mM L-glutamax (GIBCO, Invitrogen, CA, USA), and 1 mM sodium pyruvate (GIBCO, Invitrogen, CA, USA). The cell cultures were performed in a humidified incubator with 5% CO_2 at 37 °C. For MTT assay, the cells were seeded in a 96 well-plate at the concentration of 5,000 to 30,000 cells per well in 200 μL DMEM media and incubated for 18 h. Subsequently, the cells were exposed to each particle with the concentration ranging from 10 to 1000 μg/mL for 24 h. Then, 150 μL media were replaced and 20 μL of 12 mM MTT (Invitrogen, CA, USA) was added to the individual well, and the cells were kept in dark at 37 °C for 1 h. Finally, the purple crystal of deposited formazon was washed with PBS and dissolved in DMSO. The formazon absorbance at the wavelength of 540 nm was measured by an Anthos 2010 microplate reader (Biochrom Anthos Zenyth 200 Microplate Reader, MA, USA). Experiments were carried out in triplicate and two independent experiments were performed. The percentage of cell viability was calculated by comparing the O.D. of treated cells to those of the corresponding negative control.

2.7. Measurement of cytokine production

The supernatants from particle unstimulated and stimulated RAW264.7 cells were collected at 24 h and the level of interleukin (IL)-6, and tumor necrosis factor-alpha (TNF) was determined by ELISA (Biolegend, CA, USA) according to manufacturer's protocol. The absorbance of samples was measured at 450 nm using a microplate reader (Biochrom Anthos Zenyth 200 Microplate Reader, MA, USA).

3. Results and discussion

3.1. Nanocomposite synthesis and characterization

Different sizes of nanocomposites were synthesized by a three-step process: thermal decomposition of iron-oleate complexes, formation of iron oxides-silica nanocomposites, and PPEGMA coating. Crystalline structures of the synthesized MNCs nanocomposites, silica-coated magnetic nanoparticles of two different sizes (M@S-20 and M@S-40) and silica nanosphere-magnetic nanoparticle composites of two different sizes (S-M-100 and S-M-200), were characterized by X-ray diffractometry (XRD). The resulted XRD patterns were shown in Fig. 1. Compared with the standard pattern JCPDS 19-0629 and previous studies,[27] the XRD pattern of the MNPs matched well with a crystalline structure of Fe_3O_4 or magnetite. In addition, the XRD patterns of all MNCs samples were compared with standard patterns JCPDS 19-0629 of magnetite and JCPDS 29-0085 of amorphous silica. All of M@S and S-M MNCs showed diffraction peak at 2-theta of 35.42°, 43.06° and 62.12°, indicating that these MNCs contained magnetite. The broad peaks at 2-theta of 22.48° were observed, implying that silica on these MNCs was not in its crystalline phase. The XRD results confirmed that all of MNCs contained both magnetite and amorphous silica even though different preparation steps were

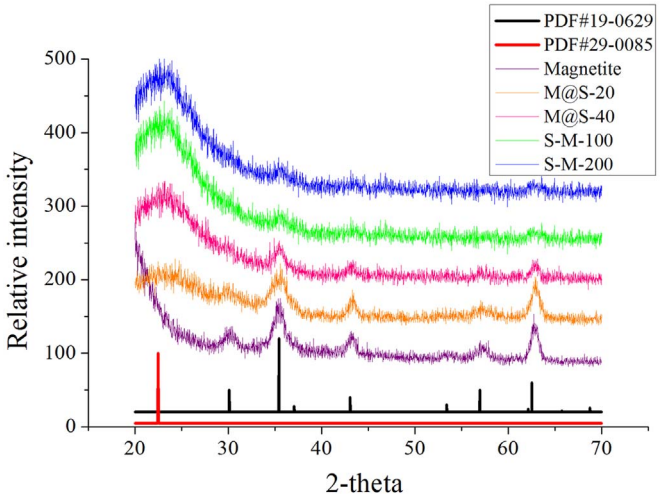

Fig. 1. The XRD patterns of the synthesized magnetic nanoparticles (MNPs) (purple), M@S (M@S-20) (orange), M@S-40 (pink) for the composites with the sizes of 20 and 40 nm in diameter, respectively, and S-M MNCs (S-M-100 (green), S-M-200 (blue) for the composites with the sizes of 100 and 200 nm in diameter, respectively. In comparison with the standard pattern files JCPDS 19-0629 (black) of magnetite and JCPDS 29-0085 (red) of amorphous silica. (For interpretation of the references to color in this figure legend, the reader is referred to the web version of this article.)

applied.

The particle sizes and morphology were observed using a TEM. The dispersity of all of PPEGMA-coated MNCs (PPEGMA-S-M and PPEGMA-M@S MNCs) are shown in Fig. 2. All of TEM images showed that individual particles were almost evenly separated, and the distances between individual particles were greater than those of MNCs without PPEGMA coated (All of MNCs shown in Fig. S1 (Supplementary)). Moreover, their surface was covered with outer layer observed as the area of lower intensity than MNCs in Fig. 2C. This area might be resulted from PPEGMA layer. All results could suggest that MNCs were completely coated with PPEGMA to form PPEGMA-MNCs. Monodispersity of these nanoparticles allowed us to further apply such magnetic nanocomposites for the study of size effect on immune responses. Additionally, electron probe micro-analyzer (EPMA) was used to estimate the ratios of magnetic nanoparticle (MNP) and silica in these nanocomposites as shown in Table S1 in Supplementary. The results from EPMA showed that silica was the major inorganic phase in all nanocomposites with the mass ratios of Fe:Si in the range of 0.027–0.086, which were calculated to the magnetite:silica mass ratios of 0.023–0.072 for all samples.

For the identification of functional groups and the confirmation of the PPEGMA coating on the MNCs surface, the comparison of IR spectra between the monomer and all of PPEGMA-coated MNCs (PPEGMA-MNCs) was investigated as shown in Fig. 3. IR stretching of terminal alkene (–C=CH) was observed at 3101 cm^{-1} for the spectrum of the PEGMA monomer, while IR spectra of all of PPEGMA-coated MNCs did not show the peak at this position. The difference between the two spectra implied that the resulted MNCs contained PPEGMA as all the monomer was transformed into the polymer. In addition, spectra of all of PPEGMA-MNCs showed the peaks at around 1700 cm^{-1} for C=O stretching (ester) and 2900 cm^{-1} for –C-H stretching. The peak at 2900 cm^{-1} of the PPEGMA-MNCs exhibited peak area more than that of MNCs without PPEGMA (nonPPEGMA-MNCs) at the same wavelength. Because the PPEGMA-MNCs mainly consist of both of –C-H bond and C=O bonds, these strong peaks of PPEGMA-MNCs indicated that significant quantity of PPEGMA were coated onto the MNCs.

In order to quantify the polymer contents in the MNCs samples, thermogravimetric analysis (TGA) of PPEGMA-coated MNCs was performed. Results from TGA as shown in Fig. 4 revealed a two-stage weight loss features. The first stage suggested that the poly(ethylene glycol) side chains was eliminated in the range of 210–290 °C, while at the other stage, which is in the range of 300–550 °C, the poly(methacrylate) was later eliminated. [28] The TGA curves of PPEGMA-MNCs showed the weight loss of 86%, 64%, 33%, and 30% for PPS-20, PPS-40, PPS-100 and PPS-200 PPEGMA-MNCs, respectively. The large decrease in PPEGMA content of the PPS-100 and PPS-200 were most likely affected from the decrease in surface area of larger particles.

Magnetic property of PPEGMA-coated MNCs was measured using a vibrating-sample magnetometer (VSM). The magnetization under different magnetic fields of magnetite (M) and PPEGMA-coated MNCs (PPS-20, PPS-40, PPS-100 and PPS-200) was as shown in Fig. 5. The saturation magnetization (Ms) of the as-synthesized magnetite is 24.34 emu/g at 25 °C, while Ms of PPEGMA-MNCs are 4.13 emu/g, 2.33 emu/g, 1.09 emu/g and 0.73 emu/g at 25 °C for the sizes of PPS-20, PPS-40, PPS-100 and PPS-200 in diameter, respectively. The decrease Ms values of the MNCs coated with PPEGMA when compared to the Ms of magnetite [29,30] were as expected as the main components of the MNCs were diamagnetic silica and PPEGMA. The differences in Ms of MNCs are likely an indicative of the difference in magnetic iron oxide component incorporated into the MNCs. Moreover, hysteresis loops were not observed in these samples, implying a characteristic feature of a superparamagnetic behavior, which is desired in many biological applications.

3.2. In vitro *studies*

Cytotoxicity of PEGMA-coated MNCs is critically important to their further application *in vivo*. In order to reduce the toxicity of MNCs, we immobilized PPEGMA on the surface of MNCs, which guarantees the hydrophilic PPEGMA to be well distributed in an aqueous environment. Moreover, the biocompatible polymer PPEGMA can improve cell uptake of PPEGMA-coated MNCs. To test cytotoxicity, the various sizes (20, 40, 100, 200 nm) and concentrations (10, 100, 1000 μg/mL) of the PPEGMA-coated MNCs were incubated with fibroblast (Fig. 6) and macrophage cells (Fig. 7), and the cell viability was determined by MTT assay. All sizes of PPEGMA-coated MNCs showed the low cytotoxicity in fibroblast as the cell viability higher than 65% albeit incubation with the highest concentration of 1000 μg/mL (Fig. 6). In macrophage (Fig. 7), the concentration of 10 and 100 μg/mL of PPEGMA-coated MNCs were partially toxic to the cells when compared to silica. At concentration of 1000 μg/mL, the sizes of 20, 40 and 100 nm of PPEGMA-coated MNCs further decreased macrophage viability, but the cytotoxicity of these nanocomposites was notably less than silica. PPEGMA-coated MNCs of 200-nm size exhibited the highest cytotoxicity when compared to the smaller sizes. However, all PPEGMA-coated MNCs produced less cytoxicity in macrophage when compared to magnetite.

The effect of MNCs on inflammatory is one importance for biological application of PPEGMA-coated MNCs. After incubating RAW264.7 cells with PPEGMA-coated MNCs, magnetite and silica for 24 h, the pro-inflammatory cytokines, IL-6 and TNF-α, were detected by ELISA as shown in Figs. 8 and 9, respectively. At concentrations of 10 and 100 μg/mL, all sizes of PPEGMA-coated MNCs and silica did not induce IL-6 production, while magnetite apparently enhanced IL-6 production. At the concentration of 1000 μg/mL, IL-6 production was highly upregulated when macrophages were incubated with PPEGMA-coated MNCs of 20- and 40-nm size (Fig. 8). On the contrary, at the concentrations of 10 and 100 μg/mL, very low level of TNF-α in macrophage was induced by PPEGMA-coated MNCs of 20-, 40- and 100-nm size, whereas the 200-nm size highly stimulated TNF-α production (Fig. 9). In addition, TNF-α production was induced in a size-dependent manner when stimulated macrophage with PPEGMA-coated MNCs at 1000 μg/mL. The results indicated that PPEGMA-coated MNCs of the size smaller than 100 nm at the concentration less than 100 μg/mL stimulated low inflammatory

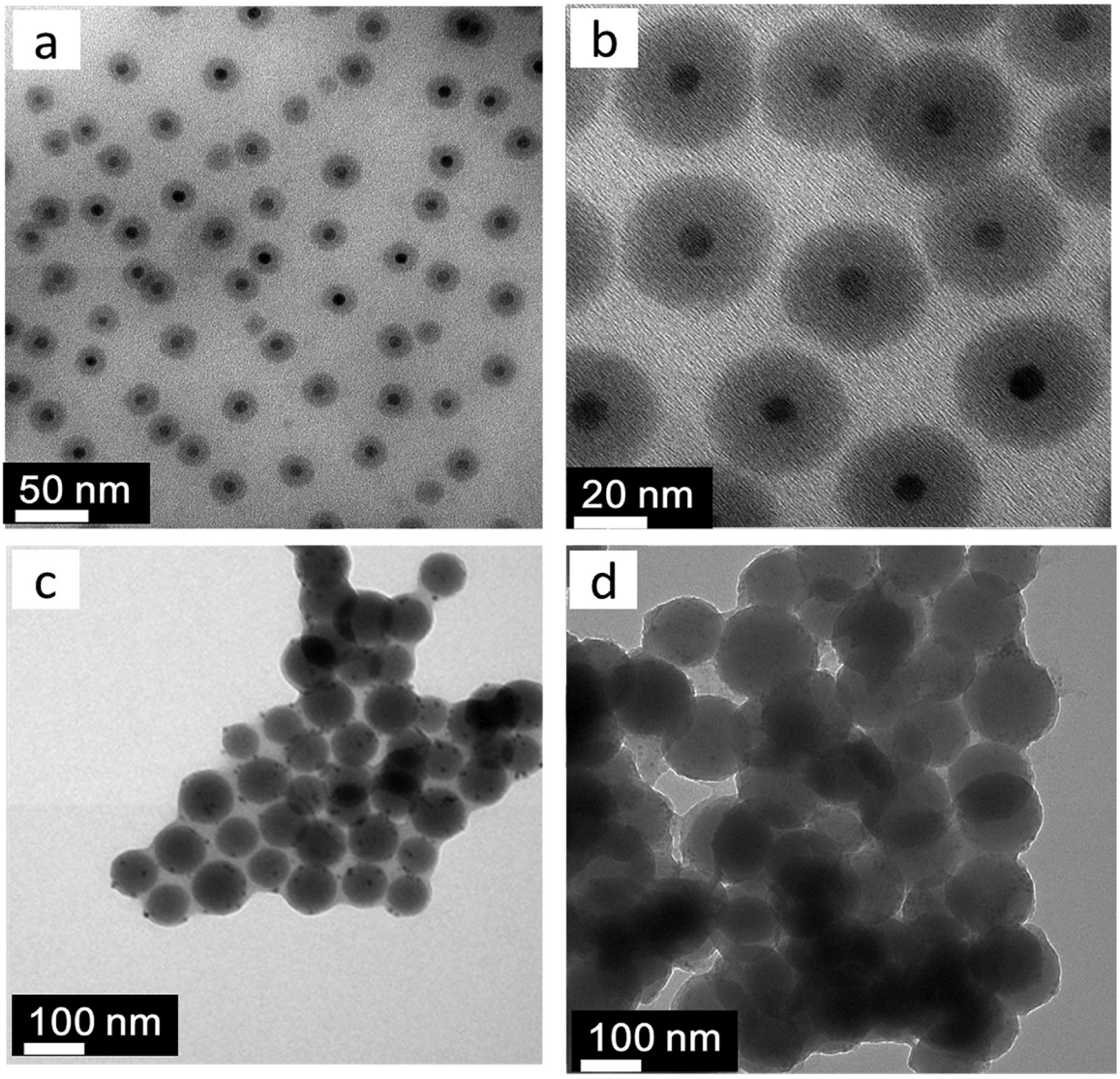

Fig. 2. TEM images of the size series of PPEGMA-coated MNCs with the diameter of (a) 24.86 ± 4.38 nm (PPS-20), (b) 45.24 ± 5.00 nm (PPS-40), (c) 98.10 ± 8.88 nm (PPS-100) and (d) 202.22 ± 6.70 nm (PPS-200).

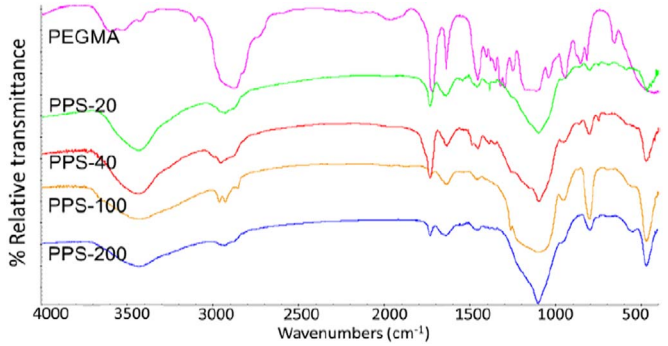

Fig. 3. IR spectra of monomer (PEGMA) and 4 samples of PPEGMA-coated MNCs, denoting PPS-20, PPS-40, PPS-100 and PPS-200, for the MNCs with the sizes of approximately 20, 40, 100 and 200 nm in diameter, respectively.

responses.

4. Conclusion

In conclusion, here we prepared different sizes of MNCs coated with PPEGMA polymer (PPEGMA-coated MNCs). PPEGMA was coated on

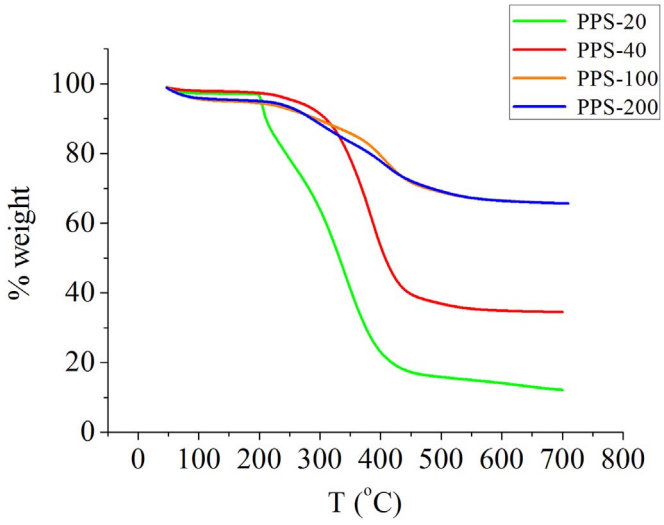

Fig. 4. TGA curves of the 4 samples of PPEGMA-coated MNCs, PPS-20, PPS-40, PPS-100 and PPS-200.

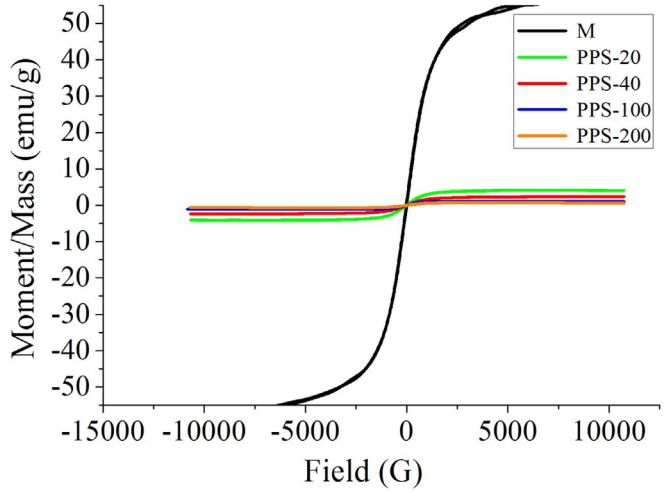

Fig. 5. Magnetization under magnetic field of as-synthesized magnetite (M) and PPEGMA-coated MNCs.

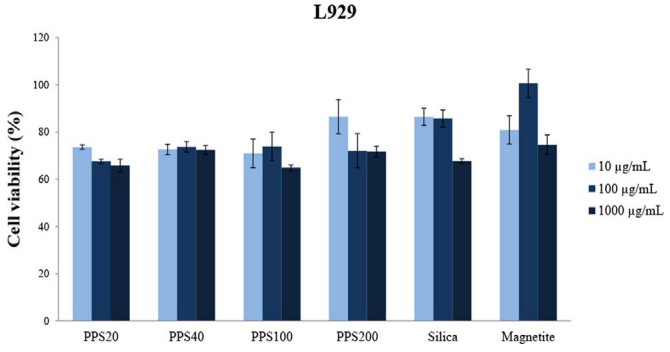

Fig. 6. Cell viability of fibroblast. L929 cells were incubated with the sizes of 20, 40, 100 and 200 nm of PPEGMA-coated MNCs, magnetite and silica at the concentrations of 10, 100 and 1000 µg/mL for 24 h. Then, the cell viability was detected by MTT assay.

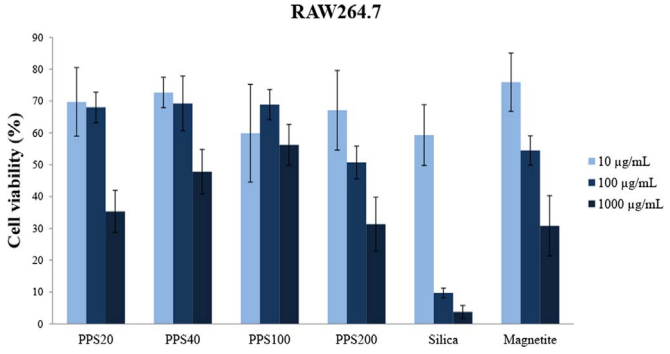

Fig. 7. Cell viability of macrophage. RAW264.7 cells were incubated with the sizes of 20, 40, 100 and 200 nm of PPEGMA-coated MNCs, magnetite and silica at the concentrations of 10, 100 and 1000 µg/mL for 24 h. Then, the cell viability was detected by MTT assay.

MNCs surface *via* ATRP. The size of PPEGMA-coated MNCs were roughly 20, 40, 100 and 200 nm, with % weight of polymer of 86%, 64%, 33%, and 30%, respectively. In addition, PPEGMA-coated MNCs with the size of smaller than 100 nm and the concentration of less than 100 µg/mL produced the low cytotoxicity and inflammatory responses when compared to magnetite. Our findings suggested that the polymer PPEGMA may decrease cytotoxicity of the magnetite and enhanced nanocomposite biocompatibility. In addition, PPEGMA-coated MNCs is possibly beneficial for biological and medical applications.

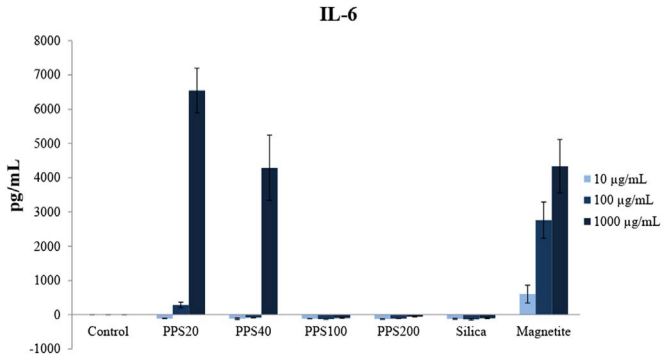

Fig. 8. IL-6 production from macrophages. RAW264.7 cells were treated with the sizes of 20, 40, 100 and 200 nm of PPEGMA-coated MNCs, magnetite and silica at the concentrations of 10, 100 and 1000 µg/mL for 24 h. Then, the IL-6 level in supernatant was measured by ELISA.

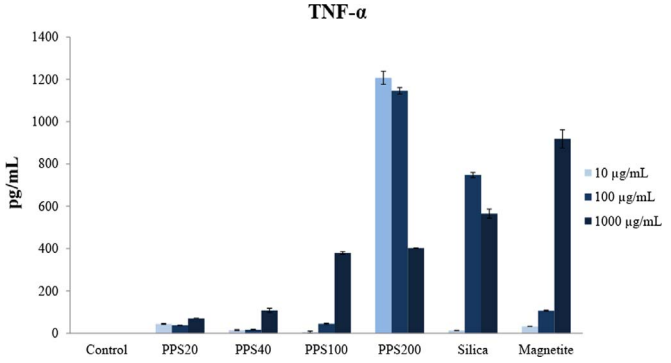

Fig. 9. TNF-α production from macrophages. RAW264.7 cells were treated with the sizes of 20, 40, 100 and 200 nm of PPEGMA-coated MNCs, magnetite and silica at the concentrations of 10, 100 and 1000 µg/mL for 24 h. Then, the TNF-α level in supernatant was measured by ELISA.

Acknowledgment

This work was financially supported by the Ratchadaphisek Somphot Endowment Fund (RES560530153-HR). Injumpa W. is supported by Science Achievement Scholarship of Thailand (SAST) and the 90th Anniversary of Chulalongkorn University Fund (Ratchadaphiseksomphot Endowment Fund).

Appendix A. Supporting information

Supplementary data associated with this article can be found in the online version at doi:10.1016/j.jmmm.2016.11.015.

References

[1] K. Yan, P. Li, H. Zhu, Y. Zhou, J. Ding, J. Shen, Z. Li, Z. Xu, P.K. Chu, RSC Adv. 3 (2013) 10598–10618. http://dx.doi.org/10.1039/C3RA40348C.
[2] T. Sen, I.J. Bruce, Microporous Mesoporous Mater. 120 (2009) 246–251. http://dx.doi.org/10.1016/j.micromeso.2008.11.012.
[3] D. Rother, T. Sen, D. East, I.J. Bruce, Nanomedicine 6 (2011) 281–300. http://dx.doi.org/10.2217/nnm.10.159.
[4] J. Wang, Z. Ali, N. Wang, W. Liang, H. Liu, F. Li, H. Yang, L. He, L. Nie, N. He, Z. Li, Sci. China Chem. 58 (2015) 1774–1778. http://dx.doi.org/10.1007/s11426-015-5483-x.
[5] R.P. Bagwe, C. Yang, L.R. Hilliard, W. Tan, Langmuir 20 (2004) 8336–8342. http://dx.doi.org/10.1021/la049137j.
[6] R.P. Bagwe, L.R. Hilliard, W. Tan, Langmuir: ACS J. Surf. Colloids 22 (2006) 4357–4362. http://dx.doi.org/10.1021/la052797j.
[7] M. Hałupka-Bryl, K. Asai, S. Thangavel, M. Bednarowicz, R. Krzyminiewski, Y. Nagasaki, Colloids Surf. B: Biointerfaces 118 (2014) 140–147. http://dx.doi.org/10.1016/j.colsurfb.2014.03.025.
[8] M. Mahmoudi, A. Simchi, M. Imani, A.S. Milani, P. Stroeve, J. Phys. Chem. B 112 (2008) 14470–14481. http://dx.doi.org/10.1021/jp803016n.
[9] H. Lee, D. Sung, J. Kim, B.-T. Kim, T. Wang, S.S.A. An, S.-W. Seo, D.K. Yi, Int. J. Nanomed. (2015) 215–225.

[10] J.-H. Ke, J.-J. Lin, J.R. Carey, J.-S. Chen, C.-Y. Chen, L.-F. Wang, Biomaterials 31 (2010) 1707–1715. http://dx.doi.org/10.1016/j.biomaterials.2009.11.026.
[11] D. Bhattacharya, M. Das, D. Mishra, I. Banerjee, S.K. Sahu, T.K. Maiti, P. Pramanik, Nanoscale 3 (2011) 1653–1662. http://dx.doi.org/10.1039/c0nr00821d.
[12] M. Mahmoudi, S. Sant, B. Wang, S. Laurent, T. Sen, Adv. Drug Deliv. Rev. 63 (2011) 24–46. http://dx.doi.org/10.1016/j.addr.2010.05.006.
[13] O.J. Osborne, S. Lin, C.H. Chang, Z. Ji, X. Yu, X. Wang, S. Lin, T. Xia, A.E. Nel, ACS Nano 9 (2015) 9573–9584. http://dx.doi.org/10.1021/acsnano.5b04583.
[14] M.K. Khaing, Oo, Y. Yang, Y. Hu, M. Gomez, H. Du, H. Wang, ACS Nano 6 (2012) 1939–1947. http://dx.doi.org/10.1021/nn300327c.
[15] M. Bañobre-López, A. Teijeiro, J. Rivas, Rep. Pract. Oncol. Radiother. 18 (2013) 397–400. http://dx.doi.org/10.1016/j.rpor.2013.09.011.
[16] M. Chastellain, A. Petri, H. Hofmann, MRS Online Proceedings Library Archive, vol. 789, 2003, N11.21 p. 14 doi: http://dx.doi.org/10.1557/PROC-789-N11.21.
[17] X. Fenghua, C. Changming, X. Fangjie, Z. Chunfu, X. Hong, X. Xuan, Y. Duanzhi, G. Hongchen, Nanotechnology 20 (2009) 405102.
[18] J.-P. Lellouche, G. Senthil, A. Joseph, L. Buzhansky, I. Bruce, E.R. Bauminger, J. Schlesinger, Journal of the American Chemical Society 127 (2005) 11998–12006. http://dx.doi.org/10.1021/ja050285l.
[19] C. Tassa, S.Y. Shaw, R. Weissleder, Accounts of chemical research 44 (2011) 842–852. http://dx.doi.org/10.1021/ar200084x.
[20] L.M. Lacava, Z.G. Lacava, M.F. Da Silva, O. Silva, S.B. Chaves, R.B. Azevedo, F. Pelegrini, C. Gansau, N. Buske, D. Sabolovic, P.C. Morais, Biophys. J. 80 (2001) 2483–2486.
[21] R.J. Benjamin, F. Michele, V. Jacob, Y.L. Angelique, Nanotechnology 18 (2007) 035603.
[22] J. Park, K. An, Y. Hwang, J.-G. Park, H.-J. Noh, J.-Y. Kim, J.-H. Park, N.-M. Hwang, T. Hyeon, Nat. Mater. 3 (2004) 891–895.
[23] D.K. Yi, S.S. Lee, G.C. Papaefthymiou, J.Y. Ying, Chem. Mater. 18 (2006) 614–619. http://dx.doi.org/10.1021/cm0512979.
[24] H. Weiwei, C. Liang, Z. Lifen, J. Xiaowu, L. Zhuang, C. Zhenping, Z. Xiulin, Nanotechnology 25 (2014) 045602.
[25] N. Insin, J.B. Tracy, H. Lee, J.P. Zimmer, R.M. Westervelt, M.G. Bawendi, ACS Nano 2 (2008) 197–202. http://dx.doi.org/10.1021/nn700344x.
[26] S.B. Yoon, Y.J. Lee, S.K. Park, H.C. Kim, H. Bae, H.M. Kim, S.G. Ko, H.Y. Choi, M.S. Oh, W. Park, J. ethnopharmacol. 125 (2009) 286–290. http://dx.doi.org/10.1016/j.jep.2009.06.027.
[27] S. Sun, H. Zeng, D.B. Robinson, S. Raoux, P.M. Rice, S.X. Wang, G. Li, J. Am. Chem. Soc. 126 (2004) 273–279. http://dx.doi.org/10.1021/ja0380852.
[28] Hu, K.G. Neoh, L. Cen, E.-T. Kang, Biomacromolecules 7 (2006) 809–816. http://dx.doi.org/10.1021/bm050870e.
[29] W. Wu, J. Changzhong, V.A.L. Roy, Nanoscale 7 (2015) 38–58. http://dx.doi.org/10.1039/C4NR04244A.
[30] L.H. Reddy, J.L. Arias, J. Nicolas, P. Couvreur, Chem. Rev. 112 (2012) 5818–5878. http://dx.doi.org/10.1021/cr300068p.